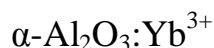


Study of the Defect Structure and Crystal-Field Parameters of

XIE Lin-Hua¹, YEUNG Yau-Yuen^{2*}¹Institute of Solid State Physics, Sichuan Normal University, Chengdu, 610066, China²Department of Science and Environmental Studies, Hong Kong Institute of Education, Hong Kong**Abstract**

The methods currently used for studying the defect structure of laser host crystals doped with transition metal or rare-earth ions have several drawbacks or limitations. This study proposes an alternative approach for obtaining optimized impurity structures using molecular dynamics calculation in conjunction with the superposition model. This new approach is specifically applied to a system named $\alpha\text{-Al}_2\text{O}_3:\text{Yb}^{3+}$, in which the simulated defect structure is used to fit the superposition model parameters directly onto the observed energy levels. Such an approach provides predicted values of crystal-field parameters, Zeeman splitting g-factor, and hyperfine structure constants. Moreover, the C_{3v} site symmetry is found to be a good approximation for the actual C_3 site of Yb^{3+} , as doped in an $\alpha\text{-Al}_2\text{O}_3$ crystal.

Keywords: molecular dynamics, crystal field, Al_2O_3 ***Corresponding author information:**

Department of Science and Environmental Studies

Hong Kong Institute of Education

10 Lo Ping Road

Tai Po, N.T.

Hong Kong, China

Fax: 852-29487676

Phone: 852-29487650

Email: yyeung@ied.edu.hk

1. Introduction

Transition metal (TM) or rare-earth (RE) ion -doped crystals, such as ruby [1], kyanite [2], lithium niobate [3,4], and zinc sulfide [5] etc are often used in making laser or optical devices. As active luminescence centers, these doped ions have important roles in the development of new material techniques. Their physical properties, including zero field-splitting and electron magnetic resonance spectra, are strongly dependent on or influenced by the local structures of the impurity-doped systems. As a result, these structures have been intensively studied over the last two to three decades. Extended X-ray absorption fine structure (EXAFS) is widely used for determining crystal structures because it is suitable for all types of atoms and ions. However, impurity concentrations lower than 100 ppm are difficult to detect. Furthermore, the EXAFS technique cannot detect bond length variations (ΔR) less than 0.03\AA . By contrast, optical and electron paramagnetic resonance (EPR) spectra are much more sensitive because they can detect impurities as low as 1 ppm and ΔR as small as 0.001\AA [6]. Therefore, TM or RE impurity structures have been extensively studied in the recent 20 years through optical and EPR spectra.

However, this method for determining the local structure from optical and EPR spectra has two major shortcomings. First, considering the insufficiency of spectral data, the defect structure is difficult or impossible to determine. This is especially the case for lower symmetry situations, where an overfit problem often exists, i.e., the number of fitting parameters is greater than the number of observed data. Second, the assumptions used to describe the defect structure are often arbitrary, improper, or oversimplified. For example, when TM or RE ions are doped in $\alpha\text{-Al}_2\text{O}_3$, some researchers assume the impurity center ion to move along the C_3 axis while the ligands are fixed around the impurity. Although the point group symmetry is maintained using this assumption, it is physically unacceptable that the ligands are not displaced in the distorted lattice. Other researchers assume that the ligands are movable. However, this assumption introduces an extra relaxation factor that is also arbitrary. These two shortcomings are difficult to overcome in the framework of traditional crystal field (CF) theory. In this study, an alternative approach was used to obtain an optimized impurity structure using molecular dynamics (MD) calculation. The simulated defect structure was then used to calculate the energy levels and to obtain the values of the optical parameters of a selected system named $\alpha\text{-Al}_2\text{O}_3\text{:Yb}^{3+}$.

2. Methods of scientific computation

In this study, the classical approach for MD simulation was adopted to determine the ionic positions in the defect system, which is formed by doping some impurity ions in a perfect host crystal. Figure 1 shows the defect system divided into (a) an inner region I with atomistic treatment for ionic relaxation and (b) an outer region II approximated as a harmonic continuum. The total energy E is given by [7, 8]:

$$E = E_I(\mathbf{R}) + E_{int}(\mathbf{R}, \mathbf{u}) + E_{II}(\mathbf{u}) \quad (1)$$

where E_I and E_{II} denote the energy for regions I and II, respectively, and the energy for the interaction between ions in these two regions is represented by E_{int} . \mathbf{R} represents the independent coordinates of the ions in region I, whereas \mathbf{u} indicates the ionic displacements in region II. Under the harmonic continuum approximation, the energy for region II can be written as:

$$E_{II}(\mathbf{u}) = \frac{1}{2} \mathbf{u}^T \cdot \mathbf{A} \cdot \mathbf{u} \quad (2)$$

where \mathbf{A} is a force matrix describing the second derivative of the total potential. At equilibrium displacement \mathbf{u}_o , the following equation holds for every ion in region II:

$$\left. \frac{\partial E}{\partial \mathbf{u}} = \frac{\partial E_{int}(\mathbf{R}, \mathbf{u})}{\partial \mathbf{u}} \right|_{\mathbf{u}=\mathbf{u}_o} + \mathbf{A} \cdot \mathbf{u} = 0 \quad (3)$$

When the above expression of matrix \mathbf{A} is substituted into Eq. (2), which is then substituted into Eq. (1),

we obtain the following equation:

$$E = E_I(\mathbf{R}) + E_{int}(\mathbf{R}, \mathbf{u}) - \frac{1}{2} \left. \frac{\partial E_{int}(\mathbf{R}, \mathbf{u})}{\partial \mathbf{u}} \right|_{\mathbf{u}=\mathbf{u}_o} \cdot \mathbf{u} \quad (4)$$

Obtaining the direct minimization of E in (4) is equivalent to solving the following equations when the partial derivative of E with respect to \mathbf{R} is set to zero for constant displacements and the equilibrium condition is met for every ion in region II:

$$0 = \left. \frac{dE}{d\mathbf{R}} = \frac{\partial E(\mathbf{R}, \mathbf{u})}{\partial \mathbf{R}} \right|_{\mathbf{u}} + \left. \frac{\partial E(\mathbf{R}, \mathbf{u})}{\partial \mathbf{u}} \right|_{\mathbf{R}} \cdot \frac{\partial \mathbf{u}_o}{\partial \mathbf{R}} \quad (5)$$

Several freely available classical MD programs, such as DL_POLY [9] and GULP [10–12], can be used to perform the above calculations. However, the required input parameters, such as inter-atomic potential parameters and shell model parameters, need to be obtained from ab initio quantum mechanical MD simulation, X-ray diffraction (XRD), or neutron-scattering experiments, such as lattice constants, phonon dispersion data, elastic constants, dielectric constants, etc. The steps outlined in Figure 2 can be used to fit the superposition model (SM) parameters to the optical spectra, resulting in the fitted values of CF parameters and predicted values of energy levels, EPR, and other hyperfine structure constants.

3. Results of defect calculation

The space group of α -Al₂O₃ is $R\bar{3}c$ (No. 167). Each crystal cell consists of 12 aluminum and 18 oxygen atoms. The 12 aluminum atoms are located in the Wyckoff c sites, which are equivalent to the fractional site $x/a = 0$, $y/b = 0$, and $z/c = 0.352$. The 18 oxygen atoms are in the e sites, which are equivalent to the fractional site $x/a = 0.306$, $y/b = 0$, and $z/c = 0.25$. The configuration of the atoms in the crystal cell is shown in Figure 3.

From the ab initio calculation using the software Material Studio, we obtained the optimized lattice parameters $a = 4.7602 \text{ \AA}$, $c = 12.9933 \text{ \AA}$, $\alpha = 90^\circ$, $\beta = 90^\circ$, and $\gamma = 120^\circ$. The calculated crystal structure of α -Al₂O₃ and its comparison with the experimental results obtained from neutron diffraction [13], XRD [14], and synchrotron X-ray [15] are listed in Table 1.

Table 1. Comparison of results obtained from ab initio calculations (present work) and experimental data (from literature) for the α -Al₂O₃ crystal structure

	Site	x/a	y/b	z/c	a	c	Ref
Al	12 c	0.0	0.0	0.352	4.7602	12.9933	Ab initio

		0.0	0.0	0.3523	4.7597(1)	12.9935(3)	Expt [13]
		0.0	0.0	0.35214	4.7540(2)	12.9935(1)	Expt [14]
		0.0	0.0	0.35223	4.7597(1)	12.9935(3)	Expt [15]
O	18 e	0.306	0.0	0.25			Ab initio
		0.3065	0.0	0.25			Expt [13]
		0.3065	0.0	0.25			Expt [14]
		0.30622	0.0	0.25			Expt [15]

The defect calculation was conducted using the MD program GULP [10–12] in a high-performance computing system with 32 CPUs. In the defect system (Figure 1), region 1 contains 222 ions and region 2 contains 2385 ions. Allowing the Yb^{3+} ion to substitute on one of the Al^{3+} sites and be the center of the impurity cluster caused the oxygen and aluminum ions to surround the doped Yb^{3+} ion. Considering the periodic boundary condition in the MD calculation, the distance between Yb^{3+} and Yb^{3+} sites was so long that their interactions can be ignored. This assumption is valid in the present case because the doped impurities were diluted and the magnetic property of the bulk material was paramagnetic.

In the defect calculation of $\alpha\text{-Al}_2\text{O}_3:\text{Yb}^{3+}$, interatomic interactions were depicted by Buckingham's two-body potentials:

$$\phi(r) = Ae^{-r/\rho} - Cr^{-6} \quad (6)$$

Given that the crystal defect may polarize the surrounding ions, we adopted the shell model [7–8, 10–12] to consider the polarization effect. In the shell model, an atom or ion is divided into two parts, core and shell. Core charge is labeled as q_c and shell charge as q_s . The core-shell interaction is represented by the harmonic vibration force constant K .

The interatomic potential and shell model parameters for the calculation of the defect structure of $\alpha\text{-Al}_2\text{O}_3:\text{Yb}^{3+}$ are shown in Table 2.

Table 2. Potential parameters and shell model parameters for the calculation of the defect structure of $\alpha\text{-Al}_2\text{O}_3:\text{Yb}^{3+}$

Buckingham's potential parameters [16]				Shell model parameters [16]			
Interactions	A/eV	ρ/eVA	C/eVA^6	ions	q_c/e	q_s/e	K/eVA^{-2}
Al–O	2409.505	0.2649	0.0	Al^{3+}	0.043	2.957	403.98
O–O	25.410	0.6937	32.32	O^{2-}	0.513	–2.513	20.53
Yb–O	991.029	0.3515	0.0	Yb^{3+}	–0.278	3.278	308.91

When the defect structure was optimized, the defect energy was 12.597 eV. The positions of the defect center Yb^{3+} core and its nearest neighboring oxygen ions are listed in Table 3. Table 3 shows that the $[\text{YbO}_6]^{9-}$ cluster exhibits C_3 symmetry, which is almost similar to C_{3v} symmetry, except that the upper and lower ligand triangles are relatively twisted, $\delta = 6.73^\circ$ [Figure 3 (b)].

Table 3. Final coordinates of the Yb³⁺ center and the nearest neighboring O²⁻ ligands

Atomic Label	Cartesian Coordinates			Polar Coordinates (origin centered at Yb)		
	x (Å)	y (Å)	z (Å)	R(Å)	θ (°)	φ (°)
Yb	0	0	4.79236	-	-	-
O1	0.82560	1.73294	5.45644	2.0312	70.92	0
O2	-1.91357	-0.15148	5.45644	2.0312	70.92	120
O3	1.08797	-1.58146	5.45644	2.0312	70.92	240
O4	-0.80093	-1.27163	3.15797	2.2203	137.40	180-δ
O5	1.50173	-0.05781	3.15797	2.2203	137.40	300-δ
O6	-0.7008	1.32944	3.15797	2.2203	137.40	60-δ

4. Energy level calculation

The f-shell electronic configuration of the Yb³⁺ ion was 4f¹³, which is equivalent to the 4f¹ conjugate configuration. Two-electron interaction is absent. Hence, the Hamiltonian of Yb³⁺ ion in a trigonal cluster can be simplified as follows:

$$H = H_{so} + H_{cf} \quad (7)$$

where H_{so} and H_{cf} are the spin-orbit (SO) coupling and the CF interaction terms, respectively. The 4f¹³ configuration of the free Yb³⁺ ion resulted in one term, ²F, which was split by SO coupling ($\zeta l \cdot s$) into the ground multiplet ²F_{7/2} and the excited multiplet ²F_{5/2} lying $7\zeta/2$ above, with the SO interaction parameter ζ being around 2900 cm⁻¹ for Yb³⁺ doped in various systems [17-19]. As an approximation, the [YbO₆]⁹⁻ cluster symmetry was taken as C_{3v}, i.e., δ was taken as 0°. The Hamiltonian for the CF interaction is usually parametrized as [17]:

$$H_{cf} = \sum_{kq} B_{kq} C_q^{(k)} = B_{20} C_0^{(2)} + B_{40} C_0^{(4)} + (B_{43} C_3^{(4)} - B_{43}^* C_{-3}^{(4)}) + B_{60} C_0^{(6)} \\ + (B_{63} C_3^{(6)} - B_{63}^* C_{-3}^{(6)}) + (B_{66} C_6^{(6)} + B_{66}^* C_{-6}^{(6)}) \quad (8)$$

where $C_q^{(k)}$ are normalized spherical harmonics and B_{kq} represents the CF parameters (with their complex conjugates denoted by B_{kq}^*). For the C₃ site symmetry, B_{kq} are complex parameters that are having non-zero imaginary component for q, with values of ± 3 or ± 6 , subject to the constraint that $|q| \leq k$ ($k = 2, 4, 6$). For the approximate C_{3v} site symmetry, all the imaginary components of the CF parameters become zero (i.e. $B_{kq} = B_{kq}^*$), reducing the total number of CF parameters from 9 (for the true C₃ site symmetry) to 6. Furthermore, B_{kq} can be determined from the SM [20, 21]:

$$B_{kq} = (-1)^q \sum_L \bar{B}_k(R_L) C_{-q}^{(k)}(\theta_L, \varphi_L) \quad (9)$$

where the summation is taken over all ligands L. The SM intrinsic parameters $\bar{B}_k(R_L)$ can be expressed in the power law form as [20]:

$$\bar{B}_k(R_L) = \bar{B}_k(R_0) \left(\frac{R_0}{R_L} \right)^{t_k} \quad (10)$$

where R_0 is the reference distance, i.e., the average ligand distance (2.1258 Å). The power-law exponents have the approximate values of $t_2=5$, $t_4=6$, and $t_6=10$ for several ionic bonds [18, 20].

By conducting the SM fit of the three SM intrinsic parameters to the seven experimental data of Yb^{3+} optical spectra (Table 4), we obtained their fitted values and the CF parameters, as calculated from Eq. (9) for the true C_3 and approximate C_{3v} sites (Table 5). The average energy was also used as an additional adjustable parameter in the fit, and there were no other free-ion parameters except for the SO coupling parameter which can also be taken as an adjustable parameter.

Table 4. Results of the SM fit for experimental energy levels (in cm^{-1}) of $\alpha\text{-Al}_2\text{O}_3:\text{Yb}^{3+}$

State	Exp. [22]	True C_3 site	Approx. C_{3v} site
${}^2F_{7/2}$	0	-7	-2
	337	360	341
	550	541	532
	1020	1026	1047
${}^2F_{5/2}$	10252	10229	10245
	10467	10541	10504
	11120	11055	11079

Table 5. Values of CF and SM parameters (in cm^{-1}) for the SM fit of the Yb^{3+} optical spectra in the true C_3 and approximate C_{3v} sites

Parameter	True C_3 site	Approx. C_{3v} site
B_{20}	-585	-580
B_{40}	-688	-953
B_{43}	-2103 - i242	-2127
B_{60}	36.2	59.7
B_{63}	67.7 - i26.7	108
B_{66}	153 + i5.3	155
\bar{B}_2	1116	1106
\bar{B}_4	899	969
\bar{B}_6	92.0	65.8

5. Discussion and conclusion

In this study, the MD method and the traditional CF theory were combined in conjunction with the SM to study the optical spectrum of $\alpha\text{-Al}_2\text{O}_3:\text{Yb}^{3+}$. In the MD calculation, the parameters in the potential

functions were determined by ab initio calculations or experiments, and the procedures for optimizing the structure were obtained by minimizing the energy of the defect system. No hypothesis or extra parameters were used to determine the local structure of the doped impurity. In this sense, the simulated defect structure of the impurity-doped system is reliable. Table 4 shows that the optical spectrum can be well explained using the MD-calculated structure and CF theory. In addition, the calculated values of the SM parameters were obtained for the oxygen ligands in Yb^{3+} ion. The C_{3v} site symmetry was found to be a good approximation given the closeness of the SM and CF parameters obtained from the two sets of fit in Table 5 (which also shows the allowed or non-zero values of the CF parameters B_{kq}) and the small values of the imaginary CF parameter components. We also tried to consider the SO coupling parameter ζ as adjustable, but the fitted value of $\zeta=2889 \text{ cm}^{-1}$ which was quite close to the literature average value of 2900 cm^{-1} [17-19] did not show significant improvement compared with using other adjustable power-law exponents.

No EPR spectral data are available for the $\alpha\text{-Al}_2\text{O}_3:\text{Yb}^{3+}$ system. However, based on the spin Hamiltonian theory [19], we obtained the Zeeman splitting parameters $g_{\parallel}=1.58$ and $g_{\perp}=3.49$ for the ground states by complete diagonalization procedure calculation using the CF parameters for the approximate C_{3v} . Using the dipolar hyperfine structure constants $P(^{171}\text{Yb})\approx 388\times 10^{-4} \text{ cm}^{-1}$ and $P(^{173}\text{Yb})\approx -107\times 10^{-4} \text{ cm}^{-1}$ [19], then $|A_{\parallel}(^{171}\text{Yb})|=409\times 10^{-4} \text{ cm}^{-1}$, $|A_{\perp}(^{171}\text{Yb})|=901\times 10^{-4} \text{ cm}^{-1}$, $|A_{\parallel}(^{173}\text{Yb})|=112\times 10^{-4} \text{ cm}^{-1}$, and $|A_{\perp}(^{173}\text{Yb})|=246\times 10^{-4} \text{ cm}^{-1}$ are predicted for future comparison with experimental data.

Acknowledgement

Financial support from the Hong Kong Institute of Education is gratefully acknowledged. This work was supported by the Doctoral Scientific Fund Project of the Ministry of Education of China (No. 20115134120004).

References

- [1] M. G. Zhao, J. Chem. Phys., 109, 8003 (1998)
- [2] Y.Y. Yeung, J. Qin, Y.M. Chang, C. Rudowicz, Phys. & Chem. Minerals, 21, 526 (1994)
- [3] M.G. Zhao, Y. Lei, J. Phys.: Condense. Matter, 9, 529 (1997)
- [4] L.H. Xie, P. Hu, P. Huang, J. Phys. & Chem. Solids, 66, 918 (2005)
- [5] Hou Shili, Yeung Yau Yuen, Mao Huibing, Wang Jiqing, Zhu Ziqiang, J. Phys. D: Appl. Phys., 42, 215105 (2009)
- [6] M.G. Zhao, M. Chiu, Phys. Rev B, 52, 10043 (1995)
- [7] Y.Y. Yeung, D.J. Newman, J. Phys. C: Solid State Phys. 21, 537(1988)
- [8] C.R.A. Catlow, R. James, W.C. Mackrodt, R.F. Stewart, Phys. Rev. B25, 1006 (1982)
- [9] W. Smith, T. Forester, I.T. Todorov, The DL POLY Classic User Manual, (2012) http://www.ccp5.ac.uk/DL_POLY_CLASSIC/MANUALS/USRMAN.pdf. Accessed 30 Nov 2012.
- [10] J.D. Gale, JCS Faraday Trans., 93 629 (1997)

- [11] J.D. Gale, *Phil. Mag. B*, 73, 3 (1996)
- [12] J.D. Gale, A.L. Rohl, *Mol. Simul.*, 29, 291 (2003)
- [13] D.M. Töbrens, N. Stüßer, K. Knorr, H.M. Mayer, G. Lampert, Berlin Neutron Scattering Center Materials Science Forum 378-381, 288 (2001)
- [14] M. Oetzel and G. Heger, *J. Appl. Crystall.* 32, 799 (1999)
- [15] E. N. Maslen, V. A. Streltsov, N. R. Streltsova, N. Ishizawa, Y. Satow, *Acta Cryst. B*49, 973 (1993)
- [16] T.S. Bush, J.D. Gale, C.R.A. Catlow and P.D. Battle, *J. Mater. Chem.*, 4, 831 (1994)
- [17] B.G. Wybourne, *Spectroscopic Properties of Rare Earths*, Wiley Inc, New York, 1965.
- [18] W.C. Zheng, H.G. Liu, P. Su, Y.G. Yang, *Spectrochim. Acta A* 84, 164 (2011).
- [19] A. Abragam, B. Bleaney, *Electron paramagnetic resonance of transition metal ions*, Oxford: Clarendon, 1970.
- [20] D.J. Newman, B. Ng, *Rep. Prog. Phys.* 52, 699 (1989).
- [21] W.L. Yu, *J. Phys.: Condens. Matter* 6, 5105 (1994).
- [22] J.K.Krebs, U.Happek, *J. Lumin.* 94–95, 65 (2001).

Figure 1. Defect structure for molecular dynamics simulation divided into two regions.

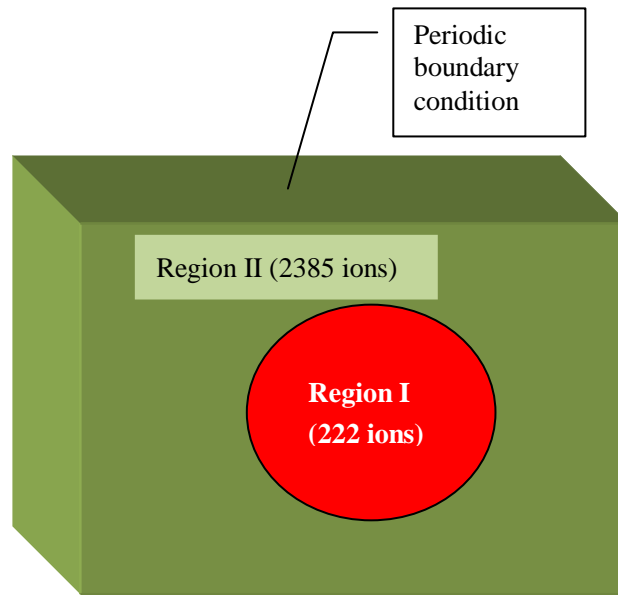


Figure 2. Flow chart of the semi-empirical approach for incorporating defect-induced lattice relaxation into the analysis of optical and EPR data

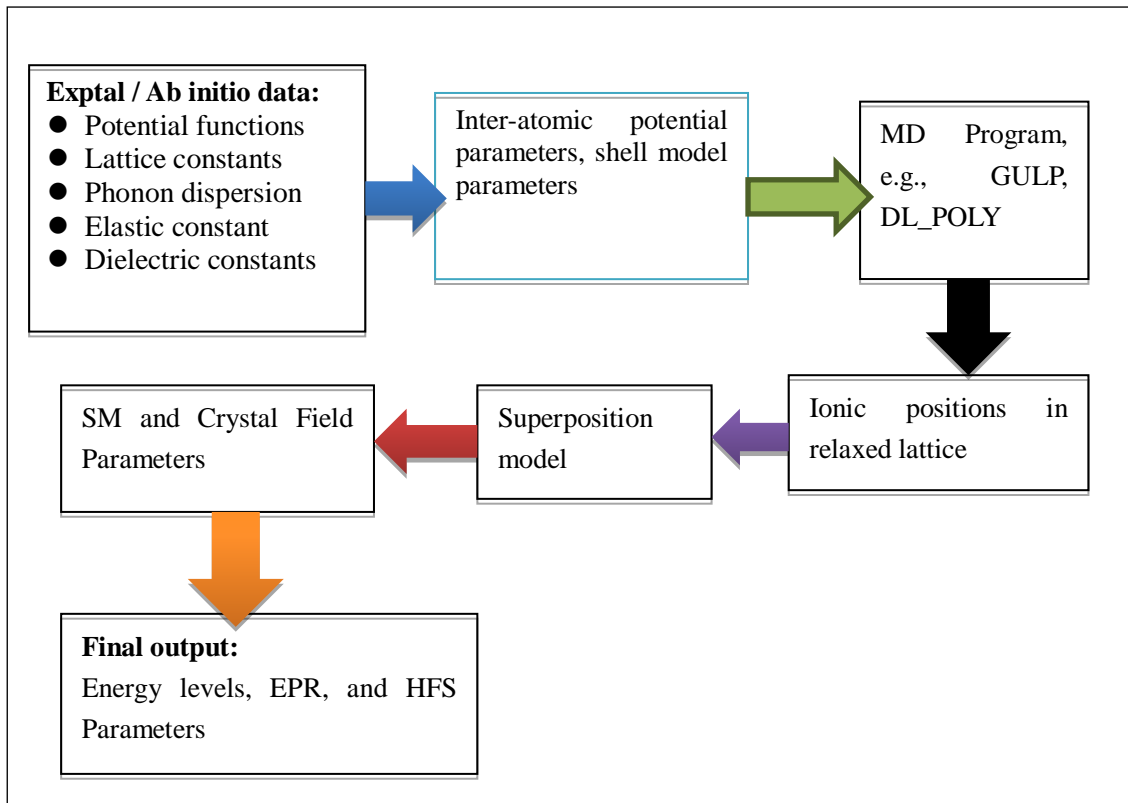


Figure 3: (a) Configuration of the α -Al₂O₃ crystal cell and (b) the coordinates frame and neighboring oxygen ligands of Yb³⁺, as doped in the α -Al₂O₃ lattice

